Key comparison BIPM.RI(I)-K2 of the air-kerma standards of the ARPANSA, Australia, and the BIPM in low-energy x-rays

D T Burns[1], C Kessler[1], D Butler[2], S Shoyookhi[2], M Hanlon[2]

[1] Bureau International des Poids et Mesures, Pavillon de Breteuil, F-92312 Sèvres CEDEX
[2] Australian Radiation Protection and Nuclear Safety Agency, Yallambie, Victoria, Australia

Abstract A key comparison has been made between the air-kerma standards of the ARPANSA, Australia, and the BIPM in the low-energy x-ray range. The results show the standards to agree at the level of the expanded uncertainty of the comparison of 9 parts in 10^3 (22 parts in 10^3 at 10 kV). The results are analysed and presented in terms of degrees of equivalence, suitable for entry in the BIPM key comparison database.

1. Introduction

An indirect comparison has been made between the air-kerma standards of the Australian Radiation Protection and Nuclear Safety Agency (ARPANSA), Australia, and the Bureau International des Poids et Mesures (BIPM) in the x-ray range from 10 kV to 50 kV. Two parallel-plate ionization chambers were used as transfer instruments. The measurements at the BIPM took place in March and April 2021 using the reference conditions recommended by the CCRI as described in Kessler and Burns (2018). Final data from the ARPANSA were received in July 2022.

2. Determination of the air-kerma rate

For a free-air ionization chamber standard with measuring volume *V*, the air-kerma rate is determined by the relation

$$\dot{K} = \frac{I}{\rho_{\mathrm{air}} V} \frac{W_{\mathrm{air}}}{e} \frac{1}{1 - g_{\mathrm{air}}} \prod_i k_i \tag{1}$$

where ρ_{air} is the density of air under reference conditions, *I* is the ionization current under the same conditions, W_{air} is the mean energy expended by an electron of charge *e* to produce an ion pair in air, g_{air} is the fraction of the initial electron energy lost through radiative processes in air, and $\Pi\, k_{\mathrm{i}}$ is the product of the correction factors to be applied to the standard.

The value used for ρ_{air} at each laboratory is given in Table 1. For use with this dry-air value, the ionization current measured for the standard must be corrected for humidity and for the difference between the density of the air of the measuring volume at the time of measurement and the value given in the table[1]. The value used for W_{air}/e is that recommended in ICRU Report 90 (ICRU 2016) for dry air, also given in Table 1.

3. Details of the standards

Both free-air chamber standards are of the conventional parallel-plate design. The BIPM air-kerma standard is described in Boutillon *et al.* (1969) and the changes made to certain correction factors are given in Burns (2004), Burns and Kessler (2009) and Burns *et al.* (2009). Implementation of the recommendations of ICRU Report 90 (ICRU 2016) is reported in Burns and Kessler (2018). The ARPANSA standard is described in Hargrave (1971) and in the report of the previous

[1] For an air temperature $T \sim 293$ K, pressure *P* and relative humidity ~50 % in the measuring volume, the correction for air density for the standard involves a temperature correction T / T_0, a pressure correction P_0 / P and a humidity correction $k_{\mathrm{h}} = 0.9980$.

comparison with the BIPM (Burns *et al.* 2010). For that comparison the correction factors for the standard were based on Lye *et al.* (2009). For the present comparison, new correction factors were adopted as well as changes made following ICRU Report 90. The main dimensions, the measuring volume and the polarizing voltage for each standard are shown in Table 2.

Table 1. Physical constants used in the determination of the air-kerma rate

Constant	Value	u_i [a]
ρ_{air} [b]	1.2045 kg m^{-3}	0.0001
ρ_{air} [c]	1.2047 kg m^{-3}	0.0002
W_{air} / e	33.97 J C^{-1}	0.0035

[a] u_i is the relative standard uncertainty.
[b] Density of dry air at T_0 = 293.15 K and P_0 = 101.325 kPa adopted at the BIPM.
[c] Density of dry air at T_0 = 293.15 K and P_0 = 101.325 kPa adopted at the ARPANSA.

Table 2. Main characteristics of the standards

Standard	BIPM L-01	ARPANSA
Aperture diameter / mm	9.941	4.9879
Air path length / mm	100.0	85.0
Collecting length / mm	15.466	20.197
Electrode separation / mm	70	60
Collector width / mm	71	80
Measuring volume / mm^3	1200.4	394.65
Polarizing voltage / V	1500	3000

4. The transfer instruments

4.1 Determination of the calibration coefficient for a transfer instrument

The air-kerma calibration coefficient N_K for a transfer instrument is given by the relation

$$N_K = \frac{\dot{K}}{I_{tr}} \tag{2}$$

where $\dot{K}$ is the air-kerma rate determined by the standard using (1) and I_{tr} is the ionization current measured by the transfer instrument and the associated current-measuring system. The current I_{tr} is corrected to the standard conditions of air temperature, pressure and relative humidity chosen for the comparison (T = 293.15 K, P = 101.325 kPa, RH = 50 %). No humidity correction is applied to the current measured using transfer instruments, on the basis that the BIPM laboratory is maintained with a relative humidity in the range from 40 % to 55 % and the ARPANSA laboratory remained in the range from 35 % to 67 %.

To derive a comparison result from the calibration coefficients $N_{K,BIPM}$ and $N_{K,NMI}$ measured, respectively, at the BIPM and at a national metrology institute (NMI), differences in the radiation qualities must be taken into account. Normally, each quality used for the comparison has the same nominal generating potential and similar filtration at each institute, but the half-value layers

(HVLs) can differ appreciably. A radiation quality correction factor k_Q is derived for each comparison quality Q. This corrects the calibration coefficient $N_{K,\mathrm{NMI}}$ determined at the NMI into one that applies at the 'equivalent' BIPM quality and is derived by interpolation of the $N_{K,\mathrm{NMI}}$ values in terms of log(HVL). The comparison result at each quality is then taken as

$$R_K = \frac{k_Q N_{K,\mathrm{NMI}}}{N_{K,\mathrm{BIPM}}} \; . \tag{3}$$

In practice, the half-value layers normally differ by only a small amount and k_Q is close to unity.

4.2 Details of the transfer instruments

Two thin-window parallel-plate ionization chambers belonging to the ARPANSA, type PTW 23344, serial numbers 0858 and 0967, were used as transfer instruments for the comparison. These two chambers were also used for the previous indirect comparison carried out in 2008 (Burns *et al.* 2010). Their main characteristics are given in Table 3. For positioning at the reference distance, the front face of the chamber casing was positioned in the reference plane.

Table 3. Main characteristics of the transfer chambers

Chamber type	PTW 23344
Window material	Polyethylene
Window thickness / mg cm^{-2}	2.5
Nominal volume / cm^3	0.2
Collector diameter / mm	13
Cavity height / mm	1.5
Polarizing potential [a] / V	300

[a] At the ARPANSA, the chambers were calibrated with +300 V applied to the collector. At the BIPM, this arrangement is not possible and –300 V was applied to the chamber entrance window.

5. Calibration at the BIPM

5.1 The BIPM irradiation facility and reference radiation qualities

The BIPM low-energy x-ray laboratory houses a high-stability generator and a tungsten-anode x-ray tube with an inherent filtration of 1 mm beryllium. A beryllium filter of thickness 2.16 mm is added for all radiation qualities to compensate for the decrease in filtration that occurred when the original BIPM x-ray tube (with a beryllium window of approximately 3 mm) was replaced in 2000; the added thickness was determined experimentally to give a half-value layer (HVL) at 10 kV matching that of the original x-ray tube. A voltage divider is used to measure the generating potential, which is stabilized using an additional feedback system of the BIPM. Rather than use a transmission monitor, which might introduce its own variability, the anode current is measured and the ionization chamber current is normalized for any deviation from the reference anode current. The standard deviation of repeat air-kerma rate determinations over many months is typically 3 parts in 10^4. The radiation qualities used in the range from 10 kV to 50 kV are those recommended by the CCRI and are given in Table 4 in ascending HVL from left to right.

The irradiation area is temperature controlled at around 20 °C and is stable over the duration of a calibration to better than 0.1 °C. Two calibrated thermistors measure the temperature of the ambient air and the air inside the BIPM standard. Air pressure is measured by means of a calibrated barometer.

Table 4. Characteristics of the BIPM reference radiation qualities

Radiation quality	10 kV	30 kV	25 kV	50 kVb	50 kVa
Generating potential / kV	10	30	25	50	50
Additional Al filtration / mm	0	0.2082	0.3723	1.0082	3.989
Al HVL / mm	0.037	0.169	0.242	1.017	2.262
$(\mu/\rho)_{air}$[a] / $cm^2\ g^{-1}$	14.83	3.66	2.60	0.75	0.38
$\dot{K}_{BIPM}$ / mGy s^{-1}	1.00	1.00	1.00	1.00	1.00

[a] Measured for an equivalent air-path length of 100 mm using a variable-pressure tube.

5.2 BIPM standard and correction factors

The reference plane for the BIPM standard was positioned at 500 mm from the exit window, with a reproducibility of 0.03 mm. The standard was aligned laterally on the beam axis to an estimated uncertainty of 0.1 mm. The beam diameter in the reference plane is 84 mm for all radiation qualities.

For the calibration of transfer chambers, measurements using the BIPM standard were made using positive polarity only. A correction factor of 1.0005 is applied to correct for the known polarity effect in the standard (see Table 5). The leakage current for the BIPM standard was measured to be less than 1 part in 10^4.

The correction factors applied to the ionization current measured at each radiation quality using the BIPM standard, together with their associated standard uncertainties, are given in Table 5.

The largest correction is that due to the attenuation of the x-ray fluence along the air path between the reference plane and the centre of the collecting volume. The corresponding correction factor k_a is evaluated using the measured mass attenuation coefficients for air $(\mu/\rho)_{air}$ given in Table 4. In practice, the values used for k_a take account of the temperature and pressure of the air in the standard.

Two new correction factors, k_{ii} and k_W, are implemented following the recommendations of ICRU Report 90 (ICRU 2016) and presented as the product $k_{ii}k_W$ by Burns and Kessler (2018). Both correction factors are related to the mean energy expended in dry air per ion pair formed, W_{air}. The initial ionization correction factor k_{ii} accounts for the fact that the definition of W_{air} does not include the charge of the initial charged particle, while the correction factor k_W accounts for the rapid increase in the value of W_{air} at electron energies below around 10 keV.

5.3 Transfer chamber positioning and calibration at the BIPM

The reference point for each chamber was positioned in the reference plane with a reproducibility of 0.03 mm. Each transfer chamber was aligned laterally on the beam axis to an estimated uncertainty of 0.1 mm. The leakage current was measured before and after each series of ionization current measurements and a correction made using the mean value. The relative leakage current for each chamber was typically 6 parts in 10^4 (8 fA) and stable over the duration of the comparison.

The calibration procedure involves measurements with a transfer chamber and with the standard at a given radiation quality before proceeding to the next quality, with a period of typically

10 minutes following a change of quality to allow the generator and tube to stabilize (longer for the 50 kVa quality). For each of the transfer chambers at each radiation quality, the relative standard uncertainty of the mean ionization current was typically below 2 parts in 10^4. Based on the results of repeat calibrations including chamber repositioning, an uncertainty component of 5 parts in 10^4 is included in Table 11 for the short-term reproducibility of the calibration coefficients determined at the BIPM.

Table 5. Correction factors and uncertainties for the BIPM standard

Radiation quality	10 kV	30 kV	25 kV	50 kVb	50 kVa	u_{iA}	u_{iB}
Air attenuation k_a [a]	1.1956	1.0451	1.0319	1.0091	1.0046	0.0002	0.0001
Photon scatter k_{sc}	0.9962	0.9972	0.9973	0.9977	0.9979	-	0.0003
Fluorescence k_{fl}	0.9952	0.9971	0.9969	0.9980	0.9985	-	0.0005
Electron loss k_e	1.0000	1.0000	1.0000	1.0000	1.0000	-	0.0001
Initial ionization k_{ii} [b] Energy dependence of W_{air} k_W [b]	0.9953	0.9968	0.9969	0.9977	0.9980	-	0.0012
Ion recombination k_s	1.0006	1.0007	1.0007	1.0007	1.0007	0.0001	0.0001
Polarity k_{pol}	1.0005	1.0005	1.0005	1.0005	1.0005	0.0001	-
Field distortion k_d	1.0000	1.0000	1.0000	1.0000	1.0000	-	0.0007
Diaphragm effects k_{dia}	0.9999	0.9995	0.9996	0.9989	0.9984	-	0.0003
Wall transmission k_p	1.0000	1.0000	1.0000	1.0000	1.0000	0.0001	-
Humidity k_h	0.9980	0.9980	0.9980	0.9980	0.9980	-	0.0003
$1 - g_{air}$	1.0000	1.0000	1.0000	1.0000	1.0000	-	0.0001

[a] Values for 293.15 K and 101.325 kPa; each measurement is corrected using the air density measured at the time.
[b] The stated values are for the product $k_{ii}k_W$, as presented in Burns and Kessler (2018).

6. Calibration at the ARPANSA

6.1 ARPANSA irradiation facility and reference radiation qualities

The low-energy x-ray facility at the ARPANSA uses a Philips RT100 x-ray unit. The unit has a tungsten-anode tube with an inherent filtration of 1 mm beryllium. The x-ray output is monitored by means of a transmission ionization chamber with a transmission thickness of nominally 2 mm of Be. The generating potential is not monitored; the generator unit was refurbished in 2018. The standard deviation of repeat calibrations of the transmission monitor over the period of a transfer chamber calibration is typically 1 part in 10^3. The characteristics of the ARPANSA realization of the CCRI comparison qualities are given in Table 6. Note that the CCRI 25 kV quality is not realized at the ARPANSA.

The irradiation area is temperature controlled around 21 °C and, despite variations of up to 2 °C during the day, is stable over the duration of a calibration to better than 0.5 °C. Two calibrated thermistors measure the temperature of the ambient air and the air inside the transmission monitor. The ARPANSA standard is not equipped with a thermometer; from time to time between measurements the internal air is monitored using a liquid-in-glass thermometer and shown to be typically within 0.2 °C of the ambient air temperature, the latter being used to normalize the ionization current. The air pressure is measured by means of a calibrated digital barometer.

Table 6. Characteristics of the ARPANSA reference radiation qualities

Radiation quality	10 kV	30 kV	50 kVb	50 kVa
Generating potential / kV	10	30	50	50
Additional Al filtration / mm	0	0.205	1.00	4.00
Al HVL / mm	0.038	0.17	1.00	2.35
$(\mu/\rho)_{air}$[a] / $cm^2\ g^{-1}$	15.0	3.45	0.77	0.38
$\dot{K}_{\mathrm{ARPANSA}}$ / $mGy\ s^{-1}$	0.9	4.8	2.6	0.6

[a] Calculated for an air-path length of 85 mm. See the discussion in Section 10.

6.2 ARPANSA standard and correction factors

The reference plane for the ARPANSA standard was positioned at 500 mm from the source, with an uncertainty of around 2 mm and a reproducibility of 0.1 mm. The standard was aligned laterally on the beam axis with a reproducibility of 0.2 mm. The beam diameter in the reference plane is 90 mm for all radiation qualities.

During the calibration of the transfer chambers, measurements using the ARPANSA standard were made using negative polarity only. The polarity correction was previously measured to be less than 1 part in 10^3 (Hargrave 1971) and verified during the present comparison. No polarity correction is applied but rather a standard uncertainty of 5 parts in 10^4 included (see Table 7). The leakage current for the ARPANSA standard including electrometer offsets was below 10 fA, corresponding to around 1 part in 10^3 for the lowest air-kerma rate, the 50 kVa quality.

The correction factors applied to the ionization current measured at each radiation quality using the ARPANSA standard, together with their associated uncertainties, are given in Table 7.

The correction factors k_a are evaluated using the calculated air-attenuation coefficients given in Table 6. In practice, the values used for k_a take account of the temperature and pressure of the air in the standard at the time of the measurements. Note that the air-attenuation coefficients used for the previous comparison were measured values (see Section 10).

6.3 Transfer chamber positioning and calibration at the ARPANSA

The reference point for each chamber was positioned in the reference plane with a reproducibility of 0.5 mm. Each transfer chamber was aligned laterally on the beam axis to an estimated uncertainty of 0.5 mm. The leakage current was measured for each measurement series and a correction applied. The leakage current including electrometer offsets was typically below 10 fA, again corresponding to around 1 part in 10^3 for the lowest air-kerma rate.

For each transfer chamber at each radiation quality, four calibrations were made before the measurements at the BIPM and three following the return of the chambers to the ARPANSA. The standard deviation of repeat calibrations for each chamber was typically 2.5 parts in 10^3, so that the mean value for each was determined to 1.0 part in 10^3. This is included in Table 11 for the uncertainty arising from the reproducibility of the calibration coefficients determined at the ARPANSA.

Table 7. Correction factors and uncertainties for the ARPANSA standard

Radiation quality	10 kV	30 kV	50 kVb	50 kVa	$u_{i\mathrm{A}}$	$u_{i\mathrm{B}}$ 10 kV	$u_{i\mathrm{B}}$ others
Air attenuation k_a [a]	1.1661	1.0360	1.0079	1.0039	-	0.010	0.0013
Photon scatter k_{sc}	0.9927	0.9949	0.9963	0.9967	-	0.0002	0.0002
Fluorescence k_{fl}	included in k_{sc}				-	0.0004	0.0004
Electron loss k_e	1.0000	1.0000	1.0002	1.0004	-	0.0003	0.0003
Initial ionization k_{ii} [b] / Energy dependence of W_{air} k_W [b]	0.9954	0.9968	0.9978	0.9980	-	0.0014	0.0010
Ion recombination k_s	1.0005	1.0005	1.0005	1.0005	-	0.0001	0.0001
Polarity k_{pol}	1.0000	1.0000	1.0000	1.0000	-	0.0005	0.0005
Field distortion k_d	1.0000	1.0000	1.0000	1.0000	-	0.0005	0.0005
Diaphragm effects k_l [c]	1.0000	1.0000	1.0000	1.0000	-	0.0001	0.0001
Humidity k_h	0.9980	0.9980	0.9980	0.9980	-	0.0003	0.0003
$1 - g_{air}$	1.0000	1.0000	1.0000	1.0000	-	0.0001	0.0001

[a] Values for 293.15 K and 101.325 kPa; each measurement is corrected using the air density measured at the time.
[b] The stated values are for the product $k_{ii}k_W$.
[c] Monte Carlo evaluation of diaphragm transmission and scatter as well as penetration through the front wall.

7. Additional considerations for transfer chamber calibrations

7.1 Ion recombination, polarity, radial non-uniformity, distance and field size

As can be seen from Tables 4 and 6, the ARPANSA and BIPM air-kerma rates differ; in the worst case, the ARPANSA air-kerma rate for the 30 kV quality is almost five times that of the BIPM. The effect of a five-fold increase has been previously measured at the BIPM for the PTW 23344 chamber type to be not more than 2 parts in 10^4 and a corresponding uncertainty for ion recombination is included in Table 12. Each transfer chamber was used with the same polarity at each laboratory and so no corrections are applied for polarity effects in the transfer chambers (noting however the different electrometer arrangement at the two laboratories as stated in the footnote to Table 3).

No correction is applied at either laboratory for the radial non-uniformity of the radiation field. For a chamber with collector diameter 13 mm the correction for the BIPM reference fields at 500 mm is only 2 parts in 10^4 and it is reasonable to assume some cancellation at the two laboratories. A corresponding uncertainty of 2 parts in 10^4 is included in Table 12.

As the reference distance is the same at both laboratories (500 mm) and the field diameters are similar (84 mm at the BIPM and 90 mm at the ARPANSA) no correction factors are applied.

7.2 Radiation quality correction factors k_Q

As noted in Section 4.1, slight differences in the realizations of the CCRI radiation qualities at the ARPANSA and the BIPM might require a correction factor k_Q. Using the HVL values determined at each laboratory as given in Tables 4 and 6, interpolation of the N_K values as described in Section 4.1 results in k_Q factors within 2 parts in 10^4 of unity. No corrections are applied and an uncertainty component of 2 parts in 10^4 is included in Table 12.

8. Comparison results

The calibration coefficients $N_{K,\mathrm{ARPANSA}}$ and $N_{K,\mathrm{BIPM}}$ for the transfer chambers are presented in Table 8. For each chamber at each radiation quality, the values $N_{K,\mathrm{ARPANSA}}$ measured before and after the measurements at the BIPM give rise to the mean value used for the final comparison result and a relative standard uncertainty s_{stab} representing the chamber stability [2].

Table 8. Calibration coefficients for the transfer chambers

Radiation quality	10 kV	30 kV	50 kVb	50 kVa
PTW 23344-0858				
$N_{K,\mathrm{ARPANSA}}$ (pre-BIPM) / Gy µC^{-1}	85.59	83.07	81.29	80.65
$N_{K,\mathrm{ARPANSA}}$ (post-BIPM) / Gy µC^{-1}	85.56	82.97	81.21	80.81
$s_{\mathrm{stab,1}}$	0.0003	0.0011	0.0009	0.0018
$N_{K,\mathrm{BIPM}}$ / Gy µC^{-1}	84.64	83.68	81.65	81.14
PTW 23344-0967				
$N_{K,\mathrm{ARPANSA}}$ (pre-BIPM) / Gy µC^{-1}	92.43	88.87	86.50	86.52
$N_{K,\mathrm{ARPANSA}}$ (post-BIPM) / Gy µC^{-1}	92.84	88.89	86.77	86.68
$s_{\mathrm{stab,2}}$	0.0041	0.0002	0.0029	0.0017
$N_{K,\mathrm{BIPM}}$ / Gy µC^{-1}	91.60	89.53	87.16	86.99

The comparison results R_K are presented in Table 9, evaluated according to Equation (3) with k_Q equal to unity. For each radiation quality the final comparison result is evaluated as the mean for the two transfer chambers. The uncertainty s_{tr} is the standard uncertainty of this mean [2], or taken as

$$s_{\mathrm{tr}} = \frac{\sqrt{s_{\mathrm{stab,1}}^2 + s_{\mathrm{stab,2}}^2}}{2} \qquad (4)$$

if this is larger (on the basis that the agreement between the comparison results for different transfer chambers should not, on average, be better than their combined stability estimated using

[2] Because of the very small sample size, the modified standard uncertainty including the appropriate *t*-factor is used, which for $n = 2$ gives $s_{\mathrm{stab}} = 1.8\, s_{\mathrm{dev.s}}/\sqrt{2}$. Likewise for s_{tr}. See Burns (2022).

$s_{stab,1}$ and $s_{stab,2}$ from Table 8). The rms value of s_{tr} for the four qualities, $s_{tr,comp}$ = 0.0014, is taken to represent the uncertainty arising from the transfer chambers and is included in Table 12.

Also given in the final row of Table 9 are the results for the ARPANSA in the previous comparison in 2008, revised for the changes made to the standards in the interim period.

Table 9. Combined comparison results

Radiation quality	10 kV	30 kV	50 kVb	50 kVa
R_K using PTW 23344-0858	1.0110	0.9921	0.9951	0.9949
R_K using PTW 23344-0967	1.0113	0.9927	0.9940	0.9955
s_{tr}	0.0014	0.0004	0.0011	0.0009
Final R_K	**1.0112**	**0.9924**	**0.9946**	**0.9952**
Updated results of 2008	1.0041	0.9958	0.9993	0.9993

9. Uncertainties

The uncertainties associated with the primary standards are listed in Table 10, and those for the transfer chamber calibrations in Table 11. The combined standard uncertainty u_c for the comparison results R_K is presented in Table 12. This uncertainty takes into account correlation in the type B uncertainties associated with the physical constants, the humidity correction and the factor $k_{ii}k_W$. Correlation in the values for k_e, k_{sc} and k_{fl}, derived from Monte Carlo calculations in each laboratory, are taken into account in an approximate way by assuming half of the uncertainty value for each factor at each laboratory. This is consistent with the analysis of the results of BIPM comparisons in low-energy x-rays in terms of degrees of equivalence described in Burns (2003).

Table 10. Uncertainties associated with the standards

Standard	BIPM L-01		ARPANSA	
Relative standard uncertainty	u_{iA}	u_{iB}	u_{iA}	u_{iB}
Ionization current	0.0002	0.0002	0.0005	0.0020
Positioning	0.0001	0.0001	-	0.0010
Volume	0.0003	0.0005	-	0.0003
Correction factors (excl. k_h)	0.0003	0.0015	-	0.0019 [a]
Humidity k_h	-	0.0003	-	0.0003
Physical constants	-	0.0035	-	0.0035
$\dot{K}$	0.0005	0.0039	0.0005	0.0046 [b]

[a] For the 10 kV quality, the value is 0.010 (see Table 7).
[b] For the 10 kV quality, the value is 0.011.

Table 11. Uncertainties associated with the calibration of the transfer chambers

Institute	BIPM		ARPANSA	
Relative standard uncertainty	u_{iA}	u_{iB}	u_{iA}	u_{iB}
$\dot{K}$	0.0005	0.0039	0.0005	0.0046 [a]
I_{tr}	0.0002	0.0002	0.0005	0.0020
Positioning of transfer chamber	0.0001	-	-	0.0020
Reproducibility	0.0005	-	0.0010	-
N_K	0.0007	0.0039	0.0012	0.0054 [a]

[a] For the 10 kV quality, the value is 0.011 (see Table 10).

Table 12. Uncertainties associated with the comparison results

Relative standard uncertainty	u_{iA}	u_{iB}
$N_{K,\mathrm{ARPANSA}}$ / $N_{K,\mathrm{BIPM}}$	0.0014	0.0041 [a]
Ion recombination	-	0.0002
Radial non-uniformity	-	0.0002
k_Q	-	0.0002
Transfer chambers $s_{tr,comp}$	0.0014	-
R_K	0.0020	0.0041 [a]
	u_c = 0.0046 [a]	

[a] Takes account of correlation in type B uncertainties. For the 10 kV quality, the value is 0.011.

10. Discussion

The comparison results R_K show the ARPANSA and BIPM standards to agree at the level of the expanded uncertainty of the comparison of 9 parts in 10^3 (22 parts in 10^3 at 10 kV). The relatively large difference between the standards at 10 kV is known to be due in some part to the adoption of calculated values for the air-attenuation correction k_a. Although the calculated values are less reliable, they are adopted for consistency with the different set of 8 beam qualities between 20 kV and 100 kV used for the ARPANSA calibration service, for which measured values are not available. The calculated values employ spectra generated to match the measured values of the HVL.

To estimate the effect of using calculated values, new measurements of k_a were made for the present comparison by moving the collecting volume 85 mm further from the aperture, as was done in 2008. The results are presented in Table 13. While for the three higher qualities the values for k_a measured in 2008 are confirmed, thus assuring the robustness of the measured values, the new value for the 10 kV quality is lower by 1.6 % from that measured in 2008. This is consistent, at least qualitatively, with the observed increase in the measured HVL from 0.032 mm to

0.038 mm. There are a number of reasons why the HVL at 10 kV might have increased, notably beam hardening through ageing, the refurbishment of the high-voltage generator in 2018 and a re-alignment of the x-ray tube.

More significantly, Table 13 shows the measured value at 10 kV to be lower than the calculated value adopted for the comparison by 2.0 %, while at 30 kV the measured value is higher by 0.25 %. The comparison results that would be obtained if the measured values for k_a were adopted are shown in the final row of the table. While the 30 kV result is more consistent with those obtained for the 50 kV qualities, the result for 10 kV is not significantly improved in absolute terms (R_K being 0.9908 rather than 1.0112) although it is closer to the results for the other qualities. The use of calculated rather than the more reliable measured values gives rise to the significant uncertainty for k_a presented in Table 7 [3].

Table 13. Measured air-attenuation correction at the ARPANSA

Radiation quality	10 kV	30 kV	50 kVb	50 kVa
Measured k_a 2008	1.1613	1.0386	1.0084	1.0048
Measured k_a 2022	1.1426	1.0386	1.0085	1.0047
Ratio measured 2022 / 2008	0.9839	1.0000	1.0001	0.9999
Calculated k_a 2022	1.1661	1.0360	1.0079	1.0039
Ratio measured 2022 / calculated	0.9798	1.0025	1.0006	1.0008
R_K using k_a measured 2022	0.9908	0.9949	0.9952	0.9960

The final row of Table 9 shows the results of the comparison carried out in 2008 using the same two transfer chambers, updated for the changes made to the standard in the interim. The results for the three higher energies are now lower than in 2008 by around 0.4 %, while the new 10 kV result is higher by 0.7 % (note that this is not related to the adoption of calculated values for k_a as the 2008 results have been updated for this change).

In principle, we can investigate these changes by looking at the stability of the individual calibration coefficients for the two transfer chambers at each laboratory. Unfortunately, the ARPANSA calibrations for the present comparison were made with the opposite polarity to that used in 2008 and the BIPM necessarily adopted this revised polarity. Nevertheless, the new BIPM results for 10 kV are within 0.2 % of the 2008 results for both chambers and it is reasonable to deduce that the 0.7 % increase in the comparison result arises largely from the change in the beam quality at the ARPANSA (independently of the change to k_a). Likewise, for the higher qualities the observed decrease of around 0.4 % is likely to be due largely to changes in the ARPANSA calibration coefficients, although this is less-clearly demonstrable.

[3] The uncertainty at 10 kV is chosen on the basis that the 2.0 % difference between the adopted value for k_a and the best estimate (that is, the measured value) is known with high confidence. It is therefore reasonable to postulate that the *expanded* uncertainty ($k = 2$) of the adopted value should encompass the measured value. This leads to a *standard* uncertainty of 1.0 %.

11. Degrees of Equivalence

The analysis of the results of BIPM comparisons in low-energy x-rays in terms of degrees of equivalence is described in Burns (2003). Following a decision of the CCRI, the BIPM determination of the air-kerma rate is taken as the key comparison reference value, for each of the CCRI radiation qualities. It follows that for each laboratory *i* having a BIPM comparison result x_i with combined standard uncertainty u_i, the degree of equivalence with respect to the reference value is the relative difference $D_i = (\dot{K}_i - \dot{K}_{\mathrm{BIPM},i}) / \dot{K}_{\mathrm{BIPM},i} = x_i - 1$ and its expanded uncertainty $U_i = 2\,u_i$. The results for D_i and U_i, expressed in mGy/Gy and including those of the present comparison, are shown in Table 14 and in Figure 1.

12. Conclusions

The key comparison BIPM.RI(I)-K2 for the determination of air kerma in low-energy x-rays shows the standards of the ARPANSA and the BIPM to agree at the level of the expanded uncertainty of the comparison of 9 parts in 10^3 (22 parts in 10^3 at 10 kV).

Tables and a graph of degrees of equivalence, including those for the ARP ANSA, are presented for entry in the BIPM key comparison database. Note that these data, while correct at the time of publication of the present report, become out of date as laboratories make new comparisons. In addition, revised validity rules for comparison data have been agreed by the CCRI(I) so that any results older than 15 years are no longer considered valid and have been removed from the KCDB. The formal results under the CIPM MRA are those available in the key comparison database (KCDB 2022).

Table 14. Degrees of equivalence

For each laboratory *i*, the degree of equivalence with respect to the key comparison reference value is the difference D_i and its expanded uncertainty U_i. Laboratory names in red indicate participation in comparison BIPM.RI(I)-K2 and blue in APMP.RI(I)-K2.

		10 kV		30 kV		25 kV		50 kVb		50 kVa	
Lab *i*	Year	D_i /(mGy/Gy)	U_i	D_i /(mGy/Gy)	U_i	D_i /(mGy/Gy)	U_i	D_i /(mGy/Gy)	U_i	D_i /(mGy/Gy)	U_i
LNE-LNHB	2009	-0.8	4.0	0.2	4.0	0.7	4.0	0.1	4.0	0.7	4.0
NIST	2010			-3.1	8.7	0.0	8.7	1.5	8.7	-2.6	8.7
ENEA	2011	-2.2	4.5	-3.2	4.5	-2.4	4.5	-2.0	4.5	-2.1	4.5
MKEH	2011	-2.7	4.7	-2.5	4.7	-1.2	4.7	-2.6	4.7	-3.4	4.7
VNIIM	2011	-3.2	5.3	-2.1	5.3	-2.2	5.3	-1.3	5.3	-0.7	5.3
VSL	2012	7.8	7.0	6.9	7.0	7.5	7.0	11.5	7.0	13.0	7.0
PTB	2014	0.3	4.9	-1.8	4.9	-2.1	4.9	-1.1	4.9	-0.6	4.9
BEV	2014	-2.0	14	-0.8	9.7	-1.3	9.7	-0.8	9.7	-1.6	9.7
NMIJ	2014	3.2	6.5	1.0	6.5	-2.3	6.5	-0.9	6.5	-2.6	6.5
CMI	2015	5.5	7.4	3.9	7.4	4.5	7.4	4.2	7.4	4.4	7.4
KRISS	2017	-1.6	4.4	-2.4	4.4	-1.6	4.4	-1.8	4.4	-1.9	4.4
NPL	2017	-12.2	4.8	-11.4	4.8	-11.1	4.8	-10.1	4.8	-9.6	4.8
NRC	2018	0.3	7.1	-2.4	7.1	-1.4	7.1	0.6	7.1	0.4	7.1
NIM	2018	-2.3	7.7	-1.1	7.7	0.5	7.7	-2.5	7.7	-3.2	7.7
GUM	2021	-5.9	5.8	5.2	5.8	1.9	5.8	3.1	5.8	1.9	5.8
ARPANSA	2022	11.2	22	-7.6	9.1			-5.4	9.1	-4.8	9.1
MNA	2008	42.0	14	25.7	14	25.9	14	34.9	14	37.0	14
BARC	2009			13.5	100	42.8	100	30.9	100	19.0	100
INER	2009	2.8	13	8.6	13	8.3	13	6.4	13	10.2	13
IAEA	2010	4.5	11	2.8	11	4.3	11	4.9	11	4.8	11

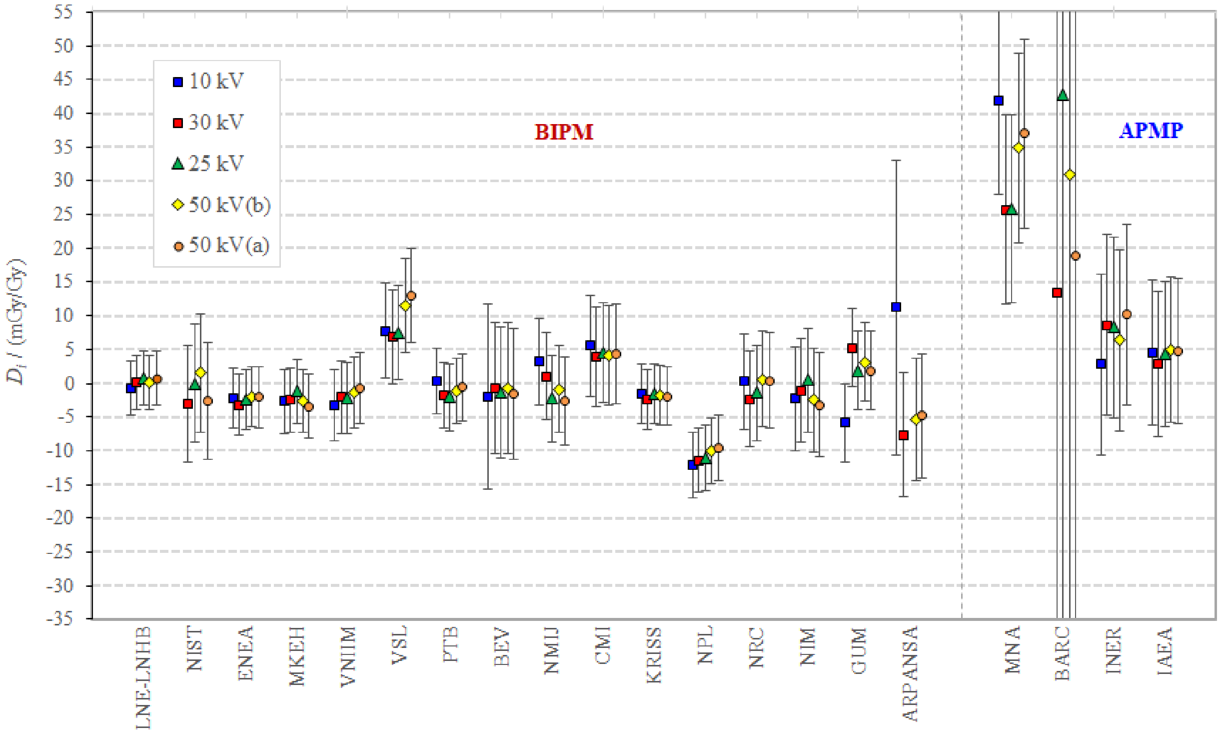

Figure 1. Degrees of equivalence for each laboratory *i* with respect to the key comparison reference value. Results to the left are for the ongoing international comparison BIPM.RI(I)-K2 and those to the right for the regional comparison APMP.RI(I)-K2 conducted between 2008 and 2010. The large uncertainty bars for the BARC are not shown (±100 mGy/Gy, see Table 14).

References

Boutillon M, Henry W H, Lamperti P J 1969 Comparison of exposure standards in the 10-50 kV x-ray region *Metrologia* **5** 1–11

Burns D T 2003 Degrees of equivalence for the key comparison BIPM.RI(I)-K2 between national primary standards for low-energy x-rays *Metrologia* **40** 06031

Burns D T 2004 Changes to the BIPM primary air-kerma standards for x-rays *Metrologia* **41** L3

Burns D T 2022 The estimation of uncertainty for small sample sizes (to be published)

Burns D T, Kessler C 2009 Diaphragm correction factors for free-air chamber standards for air kerma in x-rays *Phys Med Biol* **54** 2737–45

Burns D T, Kessler C 2018 Re-evaluation of the BIPM international dosimetry standards on adoption of the recommendations of ICRU Report 90 *Metrologia* **55** R21

Burns D T, Kessler C, Allisy P J 2009 Re-evaluation of the BIPM international standards for air kerma in x-rays *Metrologia* **46** L21–23

Burns D T, Lye J E, Kessler C, Roger P, Butler D J 2010 Key comparison BIPM.RI(I)-K2 of the air-kerma standards of the ARPANSA and the BIPM in low-energy x-rays *Metrologia* **47** 06023

Hargrave N J 1971 A Free Air Ionization Chamber for the Dosimetry of Low Energy X-rays *MSc Thesis* (Melbourne University)

ICRU 2016 Key data for ionizing-radiation dosimetry: Measurement standards and applications *J. ICRU* **14** Report 90 (International Commission on Radiation Units and Measurements: Oxford University Press)

KCDB 2022 Up-to-date results for comparison BIPM.RI(I)-K2 are available in the BIPM key comparison database at BIPM.RI(I)-K2

Kessler C, Burns D T 2018 Measuring conditions and uncertainties for the comparison and calibration of national dosimetric standards at the BIPM *Rapport* BIPM-2018/06

Lye J E, Butler D J, Webb D V 2009 Monte Carlo correction factors for the ARPANSA kilovoltage free-air chambers and the effect of moving the limiting aperture *Metrologia* **47** 11–20